



Published in final edited form as:

J Vis.; 8(10): 8.1–812. doi:10.1167/8.10.8.

Comparison of contrast-response functions from multifocal visual-evoked potentials (mfVEPs) and functional MRI responses

Jason C. Park,

Department of Psychology, Columbia University, New York, NY, USA

Xian Zhang,

Department of Radiology, and Psychology, Columbia University, New York, NY, USA

John Ferrera,

Functional MRI Research Center, Columbia University, Clinical Neuropsychology Program, CUNY Graduate Center, New York, NY, USA

Joy Hirsch, and

Departments of Radiology, Psychology, and Neuroscience, Functional MRI Research Center, Columbia University, New York, NY, USA

Donald C. Hood

Departments of Psychology and Ophthalmology, Columbia University, New York, NY, USA

Abstract

Contrast response functions (CRFs) from multifocal visual-evoked potential (mfVEP) and BOLD fMRI responses were obtained using the same stimuli to test the hypothesis of a linear relationship between the mfVEP and BOLD fMRI responses. Monocular mfVEP and BOLD fMRI responses were obtained using an 8° in diameter, dartboard pattern stimulus with reversing checkerboards. Six contrast conditions (4%, 8%, 16%, 32%, 64%, and 90%) were run. The mfVEP, largely generated in V1, was compared to the BOLD fMRI signal from V1 and extrastriate cortex. Retinotopic maps of each subject were acquired and used to localize the V1 area. For all subjects, the CRFs for the mfVEPs and BOLD fMRI responses showed good agreement, suggesting that they both share the same functional relationship with underlying neural activity. In particular, this result is consistent with the assumption that the relationship between the BOLD response and underlying neural activity is linear, although the particular linear model proposed by D. J. Heeger, A. C. Huk, W. S. Geisler, and D. G. Albrecht (2000) does not fit the results.

Keywords

V1; multifocal visual-evoked potential; mfVEP; fMRI; V1 model; contrast response function

Introduction

Functional magnetic resonance imaging (fMRI) has been widely used to study the function of the human brain. While it is clear that the physical basis of the BOLD contrast signal is the oxygenation-dependent magnetic susceptibility of hemoglobin and blood volume (Bandettini, Wong, Hinks, Tikofsky, & Hyde, 1992; Kwong et al., 1992; Ogawa, Lee, Kay, & Tank,

1990; Ogawa et al., 1992; for a review, see Logothetis & Pfeuffer, 2004; Moseley & Glover, 1995), it is less clear how this BOLD response is related to the underlying neuronal activity.

The most direct evidence concerning the relationship between the BOLD response and neuronal activity comes from studies in non-human primates comparing the intra-cortical recordings of neural signals with the BOLD fMRI responses (Logothetis, Pauls, Augath, Trinath, & Oeltermann, 2001; Shmuel, Augath, Oeltermann, & Logothetis, 2006). They recorded single- and multi-unit spiking activity (SUA and MUA) and local field potentials (LFPs) simultaneously with BOLD responses from the region of V1 and reported that the LFP and MUA correlated with the BOLD response. In general agreement, a number of studies on lower mammals support this relationship between the neural activity and the BOLD fMRI response (e.g., Kayser, Kim, Ugurbil, Kim, & König, 2004; Mathiesen, Caesar, Akgören, & Lauritzen, 1998; Niessing et al., 2005; Ogawa et al., 2000; Smith et al., 2002; Sheth et al., 2003).

Logothetis et al. (2001) also concluded that the form of the relationship between the BOLD response and the neural activity was linear. If true, this has important implications for the use of the fMRI in studying underlying human neuronal activity. However, further analysis suggested the relationship was only monotonic, not linear (Heeger & Ress, 2002; Logothetis & Wandell, 2004). Thus, while these non-human primate data strongly support a correlation between the local physiology and the local BOLD response, they do not supply strong support for a linear relationship.

Motivated by the linearity observed between the monkey's single neuron activity and the human BOLD response for V5 (Rees, Friston, & Koch, 2000), Heeger et al. (2000) took a different tack to probe the nature of the BOLD response. In particular, they compared the predictions of a model based upon recordings from monkey V1 neurons (Albrecht, 1995; Albrecht, Geisler, Frazor, & Crane, 2002; Albrecht & Hamilton, 1982; Geisler & Albrecht, 1997) to the human fMRI data from a previous experiment (Boynton, Demb, Glover, & Heeger, 1999). The contrast response functions (CRFs) predicted by the V1 model showed a striking similarity to the CRFs for the human BOLD response. As the models' response was the summed neuronal spike activity, their results support the assumption that there is a linear relationship between the BOLD response and the average underlying neuronal firing rate (Heeger et al., 2000).

More recently, Hood et al. (2006) compared the predictions of the Heeger et al. (2000) V1 model to CRFs for the human multifocal VEP (mfVEP). The mfVEP was chosen for two reasons. First, it is a measure of human cortical activity. Second, the mfVEP appears to be generated largely in V1 (Baseler, Sutter, Klein, & Carney, 1994; Hood & Greenstein, 2003; Klistorner, Graham, Grigg, & Billson, 1998; Slotnick, Klein, Carney, Sutter, & Dastmalchi, 1999; Zhang & Hood, 2004). The V1 model did not completely describe the mfVEP results. In particular, the CRFs for the mfVEP were fitted well up to about 40% contrast by the Heeger et al. V1 model, but there was a systematic deviation for higher contrasts. Hood et al. concluded that this discrepancy might be due to the violations of one or more of the model's assumptions and/or a lack of similarity between the stimulus conditions used for the neuronal recordings and the mfVEP. They suggested that CRFs for the mfVEP and fMRI should be tested under similar stimulus conditions. The purpose of the current study was to compare CRFs for mfVEP and BOLD fMRI response to identical visual stimuli. The excellent agreement found between the CRFs for the mfVEP and BOLD fMRI responses suggests that they share the same functional relationship with underlying neuronal activity.

Methods

Subjects

The seven subjects, three males and four females (mean age = 21.8 ± 3.4 years), had 20/20 corrected vision and no known visual abnormalities. Informed consent was obtained from all subjects before their participation. Procedures adhered to the tenets of the Declaration of Helsinki and the protocol was approved by the committee of the Institutional Board of Research Associates of Columbia University.

Multifocal VEP stimuli and tasks

The mfVEP display was a dartboard display comprised of a number of sectors, each with a checkerboard pattern. Both the sectors and the checks inside a sector varied in size with retinal eccentricity according to a cortical magnification factor (Baseler et al., 1994). The stimuli were projected onto a rear projection screen with a LCD video projector (Epson Model PowerLite 81p, Nagano, Japan). Because of the constraints of the projection system in the fMRI scanner, the visual angle of the dartboard pattern was restricted to a field 8° in diameter. The dartboard consisted of 24 independent sectors with three rings, 1.5° (1st ring with 4 sectors), 3.6° (2nd ring with 8 sectors), and 8° (3rd ring with 12 sectors) in diameter (Figure 1).

Each sector was an independent stimulus that reversed in contrast every 13.33 ms (screen refresh rate of 75 Hz) according to a pseudo-random m-sequence (Sutter & Tran, 1992). The mean brightness of screen was kept at 100 cd/m^2 and the contrast of dartboard stimulus was set to one of six levels: 4%, 8%, 16%, 32%, 64%, and 90%, defined as the ratio of the difference between the bright and dark checks to their sum. The mfVEP stimulus presentation was controlled by a custom built program (Zhang, 2003).

To control attention, the subject was instructed to fixate on the center cross, which changed in color at variable intervals, and count the number of times that it appeared red during the session. This task was performed during both the mfVEP recording and the fMRI scanning.

mfVEP recording

The mfVEPs were recorded from each subject on three separate days. Each day contained two sessions. Within each session, the 6 contrast conditions were arranged in random order. Each of the contrast conditions consisted of 16 segments of a 1024-step m-sequence that lasts 13.6 seconds. Figure 2A illustrates the experiment design. Note that two sessions with 6 runs repeated in the mfVEP recording. After two sessions, 32 segments for each contrast condition were completed.

The electrodes that comprise the midline channel were placed at the inion (reference) and 4 cm above the inion (active) with a forehead electrode as the ground. Additional active electrodes were placed at 4 cm lateral (left or right) to the midline and 1 cm above the inion (also active). The midline active electrode and the two lateral active electrodes were referenced to the inion electrode and created three recording channels. The positions of the active electrodes were based on anatomical considerations and chosen to optimize mfVEP recording (Hood, Zhang, Hong, & Chen, 2002). The continuous VEP record was amplified with the high and low frequency cutoffs set at 3 and 100 Hz (Grass PreAmplifier P511J, Quincy, Mass.). The mfVEP responses were filtered offline with the high and low frequency cutoffs set at 3 to 35 Hz using a fast Fourier transformation. The resistance of electrodes was less than or equal to 5 k. In general, more information about the mfVEP recording and analysis can be found in Hood et al. (2006).

The SNR measure

Special purpose software written in MATLAB (Math-works Inc., Mass.) took as its input the mfVEP records (2nd order kernels for the 24 sectors of the display) from all possible combinations of three active channels and one reference channel. The software produced the results in the form of trace arrays and performed quantitative analysis based upon the signal-to-noise ratio (SNR) of the records. In calculating the SNR, the root mean square (RMS) amplitude of the “signal window,” which contains signal plus noise, is divided by the mean RMS amplitude of the noise windows obtained in the 24 responses. The “noise window” is free of a response and of equal length to the time window of the response analysis. In particular, the signal window was 45–150 ms and the noise window was 325–430 ms. The combination of three active and one reference electrodes produced six channels of recording per each sector. SNR analyses were performed on the “best” responses from these six channels (for details, see Hood & Greenstein, 2003; Hood et al., 2002). Data from 2 participants whose maximum SNR did not reach criterion (i.e., $SNR > 2$) were excluded from further analysis. In general, more information about the mfVEP recording and analysis can be found in Hood et al. (2006).

fMRI imaging acquisition and analysis

All the participants had three fMRI scanning sessions, which were designed to be as similar as possible to the mfVEP sessions. The dartboard stimuli were the same and the subjects monitored the number of red fixation crosses as in the case of the mfVEP sessions. The stimuli were projected onto a rear projection screen by a multimedia projector (Sanyo Model No. PLC-XP30, Osaka, Japan), and the subject viewed the screen via a mirror on the head coil in the scanner.

An fMRI run lasted three minutes during which the visual stimulus was presented in six blocks. Each block lasted 13.6 seconds and was followed by a 16.4-second rest period to assure the recovery of the hemodynamic response. Each run included only one contrast condition and the order of the six runs was the same as the order of the mfVEP recording (Figure 2B).

Imaging was performed on a General Electric (Milwaukee, Wisconsin) Signal 1.5-T MRI scanner equipped with a gradient head coil ($TR = 2000$ ms, $TE = 51$ ms, $FA = 60^\circ$). Whole brain echo planar images of 21 axial slices parallel to the AC–PC line were acquired with a spatial resolution of $3.0 \times 3.0 \times 4.5$ mm. Anatomical images were obtained using a T1-weighted SPGR sequence at resolution of $1.2 \times 1.2 \times 1.2$ mm.

The functional images were filtered with a 100-second high-pass temporal filter. BOLD EPI magnitude images were spatially smoothed ($FWHM = 5$ mm). The global mean was set as covariance and removed by using regressor (Aguirre, Zarahn, & D’Esposito, 1998). A general linear model (GLM) was followed with within-subject averaging using a fixed effect model. The corrected z -statistic images for activation maps were threshold using a criterion of $Z > 2.3$. All analyses were done with SPM2 (Statistical Parametric Mapping, The Wellcome Department of Imaging Neuroscience, London, England; <http://www.fil.ion.ucl.ac.uk/spm/spm2.html>) and other customized MATLAB programs.

Retinotopic mapping

Retinotopic maps were obtained for all subjects using a 90° wedge (Engel, Glover, & Wandell, 1997) that rotated 30° clockwise every 4 seconds. These echo planar images were acquired at a resolution of $3.0 \times 3.0 \times 3.0$ mm ($TR = 2000$ ms, $TE = 54$ ms, $FA = 60^\circ$). Images were combined over two 148-second sessions. The functional imaging data were analyzed using Brain Voyager QX software (Brain Innovation B.V.). V1/V2 boundaries were drawn according to the vertical meridian near the fundus of the calcarine fissure.

Regions of interest (ROIs)

Regions of interest (ROIs) were determined for V1, and the extrastriate regions of the occipital cortex. The visual areas were further divided into rings according to eccentricity. Because there is substantial inter-subject variability in the anatomy of the visual cortex (Dougherty et al., 2003; Stensaas, Eddington, & Dobbelle, 1974), the V1 and extrastriate ROIs were obtained separately for each subject based on retinotopic mapping. Figure 3 illustrates the V1 and extrastriate (ES) areas for the average ring map from 5 subjects. To obtain these maps, the visual activation area [i.e., the z -statistic images ($z > 2.3$)] for the highest contrast levels of 90% condition was determined, and the V1 ROI was defined as the portion of the visual activation area shared with the V1 mask obtained by the retinotopic mapping procedure. The extrastriate (ES) visual area was defined as the visual activation area outside of the V1 mask, but within the occipital lobe, according to the WFU pick-atlas software (Maldjian, Laurienti, Kraft, & Burdette, 2003). The z -score from each voxel was computed and only positive z -scores, which indicated greater activation during stimulus presentation, were used for further analyses.

Comparison of signals from mfVEP and fMRI

The contrast response function (CRF) for both the fMRI and mfVEP data were fitted by an equation used to describe the CRF of V1 neurons (Albrecht et al., 2002; Naka & Rushton, 1966; Sclar, Maunsell, & Lennie, 1990). In particular,

$$R_{\text{esp}} = B + \frac{R_{\text{max}} C^\alpha}{\sigma^\alpha + C^\alpha}, \quad (1)$$

where R_{esp} is the amplitude of the response to the stimulus, B is the baseline, R_{max} is the asymptotic amplitude of the response, C is the contrast of the stimulus, α is the exponential term that alters the steepness of the CRF, and σ is the semi-saturation contrast.

Goodness of fitness

The goodness of fitness of Equation 1 was measured with the coefficient of determination, R^2 , which was calculated like below:

$$R^2 = 1 - \frac{\text{RSS}}{\text{TSS}} = 1 - \frac{\sum_{i=1}^6 (R_i - R_{i,\text{model}})^2}{\sum_{i=1}^6 (R_i - \bar{R})^2}, \quad (2)$$

where RSS is the residual sum of squares and TSS is the total sum of squares. i is the number of corresponding contrast conditions. R_i is the actual data for each contrast, and $R_{i,\text{model}}$ is the expected value from Equation 1. \bar{R} is the mean of all 6 R_i .

Results

mfVEP

Figure 4 shows the grand-average of the mfVEP responses (best channel) from all 5 subjects. Each set of 6 waveforms shows the responses to a particular sector of the dartboard display. Two sets were enlarged and shown as insets. Note that the amplitudes in the signal window (45–150 ms shown as the dashed lines) increased systemically with increase in contrast. Figure

5A shows the CRFs (i.e., the SNR of the mfVEP as a function of contrast) for one subject (S1). The thin blue lines are the results for the 3 mfVEP recording sessions. The open circles show the median values for the 3 sessions. The results for the other 4 subjects are shown in the upper row of Figure 5C. In general, the mfVEP amplitude (SNR) increased with stimulus contrast for all subjects.

Equation 1 was fitted to the medians of the 3 sessions (open circles) and displayed as the thick black lines in Figures 5A and 5C. The data were well fitted; the R^2 values were all greater than 0.9. The parameters of best fit of Equation 1 are shown in first 5 rows of Table 1. The baseline B was essentially zero for all subjects except S2 (0.83). The mean \pm SD of the semi-saturation contrast σ was $9.8\% \pm 2.7\%$ and the mean \pm SD of the maximum response R_{\max} was 3.75 ± 1.17 . The mean \pm SD of α was 1.36 ± 0.80 .

The median values (open circles) from each subject were normalized by the value for 32% contrast. These normalized values were averaged and are shown in Figure 6 as the black open circles. The black curve is the fit of Equation 1 (the other symbols and curves will be explained below). The bottom row in Table 1 shows the parameters of best fit to these pooled data. The value of R^2 was 0.94. The baseline B is almost zero and R_{\max} was 1.17. The semi-saturation point σ was 7.8% and α was close to 1.0 (1.12).

fMRI BOLD response

The activation maps of the BOLD responses from all 5 subjects are presented in Figure 7 for the 6 contrast conditions (rows) and 4 axial slices (columns). Axial slices are located from ventral to dorsal, as indicated by the slice numbers (on the top of each column). Note that the activation tended to increase with increased contrast as indicated by the increase in the size of the region in color for all the subjects.

Figure 8 shows the time course of the relative change in the BOLD obtained for the pooled data from all 5 subjects for all 3 daily sessions. Figure 8 shows a very similar pattern to the mfVEP responses in Figure 4. In particular, as contrast increases, the amplitude of both the mfVEP and BOLD fMRI responses increases with successively higher contrasts yielding progressively smaller increments in response amplitude. Of course, there is a major difference in the time scale of the mfVEP (milliseconds in Figure 4) and fMRI (seconds in Figure 8) responses.

Figure 5B shows the CRFs (i.e., mean z-score as a function of contrast) for one of the subjects (S1). The thin blue (V1) and red (ES) lines show the results for the 3 fMRI scanning sessions. The open circles are the median values for the 3 sessions. The results for the other 4 subjects are shown in the lower row (panel D) of Figure 5. In general, the BOLD responses increased with stimulus contrast for all subjects as did the mfVEP response. Note that the BOLD responses from V1 area are larger than the signals from the ES region for all subjects.

Equation 1 was fitted to the median values of the 3 sessions (open circles) and displayed as the thick black lines in Figures 5B and 5D. The data were well fitted by Equation 1; the R^2 values were high (>0.96 for V1, >0.94 for ES). The parameters estimated from Equation 1 are displayed in Tables 2 (for V1) and 3 (for ES). The baseline B values from V1 and ES were near zero. The semi-saturation contrasts σ were slightly higher in V1 than ES ($11.1\% \pm 2.5\%$ for V1; $8.3\% \pm 2.9\%$ for ES). While the B and σ parameters were similar in V1 and ES, the R_{\max} values were lower for ES (0.94 ± 0.11) than for V1 (2.49 ± 0.47). This implies that the shapes of CRF curves from two ROIs will be very similar after normalization to account for the difference of absolute signal strength.

The median fMRI values (open circles) from each of the 5 subjects were normalized by the value for 32% contrast. These normalized values were averaged and are shown in Figure 6 as the blue (V1) and red (ES) open circles. The blue and red curves are the fits of Equation 1 for V1 and ES, respectively. The parameters of the fit of Equation 1 are shown in the bottom row in Tables 2 and 3. The baseline values B were close to zero, and the R_{\max} values were 1.14 and 1.16 for V1 and ES, respectively. The semi-saturation points σ were 10.7% (for V1) and 8.6% (for ES). The values of R^2 were 1.00 (for V1) and 0.99 (for ES). The parameters of best fit to the normalized data in Figure 6 were similar for the V1 and ES regions and both were similar to the parameters of the fit to the mfVEP results as will be discussed below.

The Pearson correlation coefficients (r) between the σ values from the mfVEP and the BOLD fMRI responses were poor and not statistically significant. The r -value for the mfVEP and fMRI responses from V1 was -0.04 ($p = 0.94$), and from ES was 0.43 ($p = 0.47$).

Discussion

The purpose of the current study was to compare CRFs for mfVEP and BOLD fMRI responses to identical visual stimuli. The resulting CRFs of the mfVEP and BOLD fMRI responses showed good agreement. As seen in Figure 6, the parameters of Equation 1 were similar. The baseline B was essentially 0 in both cases; the semi-saturation contrasts were reasonably close (7.8% for SNR of mfVEP, 10.7 and 8.6% for z -scores of the BOLD fMRI responses for V1 and ES). In other words, the BOLD fMRI responses both for V1 and ES are linearly related to the mfVEP response. In general, the results suggest that fMRI and mfVEP responses share the same functional relationship with underlying neural activity. In particular, the results are consistent with the hypothesis that each is linearly related to the underlying neural activity (the linear hypothesis). Given this hypothesis, one should expect the s parameter values from the fMRI and mfVEP responses to be correlated. The poor correlations are probably due to a combination of factors including the restrict range of s values and the small number of subjects.

While past work has shown a good correlation between the BOLD response and neural activity, the evidence for linear hypothesis is less clear. As discussed above, the Logothetis et al. (2001) primate study supports a monotonic, but not a linear, relationship. Studies with lower mammals (Kayser et al., 2004; Smith et al., 2002; Thompson, Peterson, & Freeman, 2003), with monkey (Shmuel et al., 2006), and with humans (Mukamel et al., 2005) also suggested a tightly coupled, but not strictly linear, relationship. On the other hands, several studies (Arthurs, Williams, Carpenter, Pickard, & Boniface, 2000; Brinker et al., 1999; Mathiesen et al., 1998; Norup Nielsen & Lauritzen, 2001; Rees et al., 2000; Schmidt, Singer, & Galuske, 2004; Sheth et al., 2003) concluded that there was a linear relationship. However, the actual data in most of these studies do not provide strong support for this conclusion.

Heeger and his colleague (2000) also concluded there is a linear relationship between the spiking activity and BOLD fMRI response in V1. Their conclusion was based upon a comparison between a model of V1 monkey neural activity and data from a human fMRI study (Boynton et al., 1999). As the model of V1, based on a sum of V1 single unit activity, fitted the fMRI data well, they concluded that the BOLD responses were proportional to neuronal firing rates. However, as shown in Figure 9, this model does not describe the mfVEP or BOLD fMRI CRFs in the current study. Figure 9 shows the predicted CRF for the V1 model (gray curves) proposed by Heeger et al. (2000) with the CRFs from Figure 6. The dashed gray curve was pinned at a maximum response of 1.0 as in Heeger et al.'s study, while the solid gray curve was pinned at the amplitude at 32%. To better understanding the reasons for the poor fit of their model to our data, we need to examine the assumptions underlying their model.

The V1 model assumes that the BOLD response is proportional to the local firing rate (action potentials per second), averaged over a small region of cortex and a short period of time (Boynton, Engel, Glover, & Heeger, 1996; Heeger et al., 2000). However, the BOLD response may be more closely related to the synaptic activity and local field potentials than to spiking activity (Logothetis et al., 2001; Logothetis & Wandell, 2004). Perhaps it is the slow potentials that are reflected in the BOLD response and that the V1 model does not describe these slow potentials. The agreement between the BOLD and mfVEP responses in our current study supports these views. The VEP response is not generally thought to reflect spiking activity. Rather, it is largely the result of the local field potentials produced by the interplay of EPSP and IPSP activity on pyramidal cells (e.g., Schroeder, Tenke, & Givre, 1992).

Given that spiking activity and slow potentials are highly correlated (e.g., Logothetis et al., 2001; Shmuel et al., 2006), the other assumptions of the V1 model need to be examined as well. While these assumptions are not completely spelled out in the Heeger et al. study, Hood et al. (2006) claimed to make these assumptions explicit. For example, they pointed out that the V1 model must assume that the parameters of Equation 1 do not change over a range of stimulus conditions. This assumption was implied because the monkey data, upon which the model was based, and the human fMRI data, to which it was compared, were obtained with stimuli with different spatiotemporal characteristics. Support for a violation of this assumption comes from fMRI data showing that the temporal (Boynton et al., 1996) and spatial (Boynton et al., 1999) frequency of the stimuli changed the parameters of the CRFs of the BOLD response. The V1 model may need to be modified to take the spatiotemporal characteristics of the stimuli into consideration.

Conclusion

The CRFs for the mfVEP and fMRI responses to the same stimuli show good agreement at all contrast levels. They are linearly related. This result is consistent with the hypothesis that the human mfVEP and BOLD fMRI responses, at least under our stimulus conditions, are linearly related to the underlying neuronal activity, most likely the local slow potentials.

Acknowledgments

This work was supported by NIH/NEI grant EY02115.

References

- Aguirre GK, Zarahn E, D'Esposito M. The inferential impact of global signal covariates in functional neuroimaging analyses. *Neuroimage* 1998;8:302–306. [PubMed: 9758743]
- Albrecht DG. Visual cortex neurons in monkey and cat: Effect of contrast on the spatial and temporal phase transfer functions. *Visual Neuroscience* 1995;12:1191–1210. [PubMed: 8962836]
- Albrecht DG, Geisler WS, Frazor RA, Crane AM. Visual cortex neurons of monkeys and cats: Temporal dynamics of the contrast response function. *Journal of Neurophysiology* 2002;88:888–913. [PubMed: 12163540]
- Albrecht DG, Hamilton DB. Striate cortex of monkey and cat: Contrast response function. *Journal of Neurophysiology* 1982;48:217–237. [PubMed: 7119846]
- Arthurs OJ, Williams EJ, Carpenter TA, Pickard JD, Boniface SJ. Linear coupling between functional magnetic resonance imaging and evoked potential amplitude in human somatosensory cortex. *Neuroscience* 2000;101:803–806. [PubMed: 11113329]
- Bandettini PA, Wong EC, Hinks RS, Tikofsky RS, Hyde JS. Time course EPI of human brain function during task activation. *Magnetic Resonance in Medicine* 1992;25:390–397. [PubMed: 1614324]
- Baseler HA, Sutter EE, Klein SA, Carney T. The topography of visual evoked response properties across the visual field. *Electroencephalography and Clinical Neurophysiology* 1994;90:65–81. [PubMed: 7509275]

- Boynton GM, Demb JB, Glover GH, Heeger DJ. Neuronal basis of contrast discrimination. *Vision Research* 1999;39:257–269. [PubMed: 10326134]
- Boynton GM, Engel SA, Glover GH, Heeger DJ. Linear systems analysis of functional magnetic resonance imaging in human V1. *Journal of Neuroscience* 1996;16:4207–4221. [PubMed: 8753882]
- Brinker G, Bock C, Busch E, Krep H, Hossmann KA, Hoehn-Berlage M. Simultaneous recording of evoked potentials and T2*-weighted MR images during somatosensory stimulation of rat. *Magnetic Resonance in Medicine* 1999;41:469–473. [PubMed: 10204868]
- Dougherty, RF.; Koch, VM.; Brewer, AA.; Fischer, B.; Modersitzki, J.; Wandell, BA. Visual field representations and locations of visual areas V1/2/3 in human visual cortex; *Journal of Vision*. 2003. p. 1p. 586-598.<http://journalofvision.org/3/10/1/>
- Engel SA, Glover GH, Wandell BA. Retinotopic organization in human visual cortex and the spatial precision of functional MRI. *Cerebral Cortex* 1997;7:181–192. [PubMed: 9087826]
- Geisler WS, Albrecht DG. Visual cortex neurons in monkeys and cats: Detection, discrimination, and identification. *Visual Neuroscience* 1997;14:897–919. [PubMed: 9364727]
- Heeger DJ, Huk AC, Geisler WS, Albrecht DG. Spikes versus BOLD: What does neuroimaging tell us about neuronal activity? *Nature Neuroscience* 2000;3:631–633.
- Heeger DJ, Ress D. What does fMRI tell us about neuronal activity? *Nature Reviews, Neuroscience* 2002;3:142–151.
- Hood, DC.; Ghadiali, Q.; Zhang, JC.; Graham, NV.; Wolfson, SS.; Zhang, X. Contrast-response functions for multifocal visual evoked potentials: A test of a model relating V1 activity to multifocal visual evoked potentials activity; *Journal of Vision*. 2006. p. 4p. 580-593.<http://journalofvision.org/6/5/4/>
- Hood DC, Greenstein VC. Multifocal VEP and ganglion cell damage: Applications and limitations for the study of glaucoma. *Progress in Retinal and Eye Research* 2003;22:201–251. [PubMed: 12604058]
- Hood DC, Zhang X, Hong JE, Chen CS. Quantifying the benefits of additional channels of multifocal VEP recording. *Documenta Ophthalmologica* 2002;104:303–320. [PubMed: 12076018]
- Kayser C, Kim M, Ugurbil K, Kim DS, König P. A comparison of hemodynamic and neural responses in cat visual cortex using complex stimuli. *Cerebral Cortex* 2004;14:881–891. [PubMed: 15084493]
- Klistorner AI, Graham SL, Grigg JR, Billson FA. Electrode position and the multi-focal visual-evoked potential: Role in objective visual field assessment. *Australian and New Zealand Journal of Ophthalmology* 1998;26:S91–S94. [PubMed: 9685035]
- Kwong KK, Belliveau JW, Chesler DA, Goldberg IE, Weisskoff RM, Poncelet BP, et al. Dynamic magnetic resonance imaging of human brain activity during primary sensory stimulation. *Proceedings of the National Academy of Sciences of the United States of America* 1992;89:5675–5679. [PubMed: 1608978]
- Logothetis NK, Pauls J, Augath M, Trinath T, Oeltermann A. Neurophysiological investigation of the basis of the fMRI signal. *Nature* 2001;412:150–157. [PubMed: 11449264]
- Logothetis NK, Pfeuffer J. On the nature of the BOLD fMRI contrast mechanism. *Magnetic Resonance Imaging* 2004;22:1517–1531. [PubMed: 15707801]
- Logothetis NK, Wandell BA. Interpreting the BOLD signal. *Annual Review of Physiology* 2004;66:735–769.
- Maldjian JA, Laurienti PJ, Kraft RA, Burdette JH. An automated method for neuroanatomic and cytoarchitectonic atlas-based interrogation of fMRI data sets. *Neuroimage* 2003;19:1233–1239. [PubMed: 12880848]
- Mathiesen C, Caesar K, Akgören N, Lauritzen M. Modification of activity-dependent increases of cerebral blood flow by excitatory synaptic activity and spikes in rat cerebellar cortex. *The Journal of Physiology* 1998;512:555–566. [PubMed: 9763643]
- Moseley ME, Glover GH. Functional MR imaging. Capabilities and limitations. *Neuroimaging Clinics of North America* 1995;5:161–191. [PubMed: 7640883]
- Mukamel R, Gelbard H, Arieli A, Hasson U, Fried I, Malach R. Coupling between neuronal firing, field potentials, and fMRI in human auditory cortex. *Science* 2005;309:951–954. [PubMed: 16081741]
- Naka KI, Rushton WA. S-potentials from colour units in the retina of fish (Cyprinidae). *The Journal of Physiology* 1966;185:536–555. [PubMed: 5918058]

- Niessing J, Ebisch B, Schmidt KE, Niessing M, Singer W, Galuske RA. Hemodynamic signals correlate tightly with synchronized gamma oscillations. *Science* 2005;309:948–951. [PubMed: 16081740]
- Norup Nielsen A, Lauritzen M. Coupling and uncoupling of activity-dependent increases of neuronal activity and blood flow in rat somatosensory cortex. *The Journal of Physiology* 2001;533:773–785. [PubMed: 11410634]
- Ogawa S, Lee TM, Kay AR, Tank DW. Brain magnetic-resonance imaging with contrast dependent on blood oxygenation. *Proceedings of the National Academy of Sciences of the United States of America* 1990;87:9868–9872. [PubMed: 2124706]
- Ogawa S, Lee TM, Stepnoski R, Chen W, Zhu XH, Ugurbil K. An approach to probe some neural systems interaction by functional MRI at neural time scale down to milliseconds. *Proceedings of the National Academy of Sciences of the United States of America* 2000;97:11026–11031. [PubMed: 11005873]
- Ogawa S, Tank DW, Menon R, Ellermann JM, Kim SG, Merkle H, et al. Intrinsic signal changes accompanying sensory stimulation: Functional brain mapping with magnetic resonance imaging. *Proceedings of the National Academy of Sciences of the United States of America* 1992;89:5951–5955. [PubMed: 1631079]
- Rees G, Friston K, Koch C. A direct quantitative relationship between the functional properties of human and macaque V5. *Nature Neuroscience* 2000;3:716–723.
- Schmidt KE, Singer W, Galuske RA. Processing deficits in primary visual cortex of amblyopic cats. *Journal of Neurophysiology* 2004;91:1661–1671. [PubMed: 14668297]
- Schroeder CE, Tenke CE, Givre SJ. Subcortical contributions to the surface-recorded flash-VEP in the awake macaque. *Electroencephalography and Clinical Neurophysiology* 1992;84:219–231. [PubMed: 1375881]
- Scialojan G, Maunsell JH, Lennie P. Coding of image contrast in central visual pathways of the macaque monkey. *Vision Research* 1990;30:1–10. [PubMed: 2321355]
- Sheth S, Nemoto M, Guiou M, Walker M, Pouratian N, Toga AW. Evaluation of coupling between optical intrinsic signals and neuronal activity in rat somatosensory cortex. *Neuroimage* 2003;19:884–894. [PubMed: 12880817]
- Shmuel A, Augath M, Oeltermann A, Logothetis NK. Negative functional MRI response correlates with decreases in neuronal activity in monkey visual area V1. *Nature Neuroscience* 2006;9:569–577.
- Slotnick SD, Klein SA, Carney T, Sutter E, Dastmalchi S. Using multi-stimulus VEP source localization to obtain a retinotopic map of human primary visual cortex. *Clinical Neurophysiology* 1999;110:1793–1800. [PubMed: 10574294]
- Smith AJ, Blumenfeld H, Behar KL, Rothman DL, Shulman RG, Hyder F. Cerebral energetics and spiking frequency: The neurophysiological basis of fMRI. *Proceedings of the National Academy of Sciences of the United States of America* 2002;99:10765–10770. [PubMed: 12134056]
- Stensaas SS, Eddington DK, Dobelle WH. The topography and variability of the primary visual cortex in man. *Journal of Neurosurgery* 1974;40:747–755. [PubMed: 4826600]
- Sutter EE, Tran D. The field topography of ERG components in man—I. The photopic luminance response. *Vision Research* 1992;32:433–446. [PubMed: 1604830]
- Thompson JK, Peterson MR, Freeman RD. Single-neuron activity and tissue oxygenation in the cerebral cortex. *Science* 2003;299:1070–1072. [PubMed: 12586942]
- Zhang X. Simultaneously recording local luminance responses, spatial and temporal interactions in the visual system with m-sequences. *Vision Research* 2003;43:1689–1698. [PubMed: 12798150]
- Zhang, X.; Hood, DC. A principal component analysis of multifocal pattern reversal VEP; *Journal of Vision*. 2004. p. 4,32-43.<http://journalofvision.org/4/1/4/>

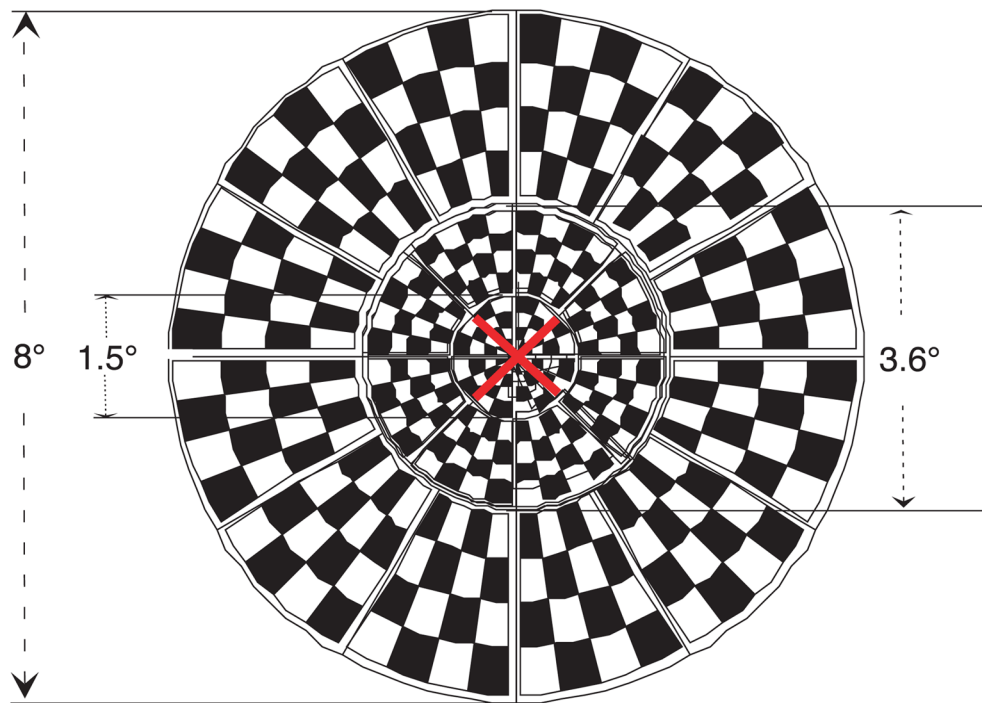


Figure 1.
The dartboard stimulus with 24 sectors used for both mfVEP recordings and fMRI scans.

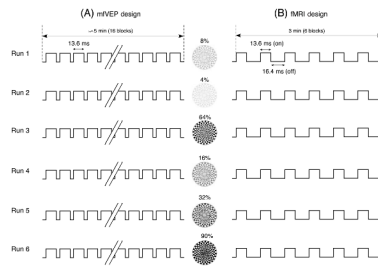


Figure 2. A sample experimental design for mfVEP (A) and fMRI (B). The order of stimulus contrasts was assigned randomly for each (e.g. 8%-4%-64%-16%-32%-90% in this case).

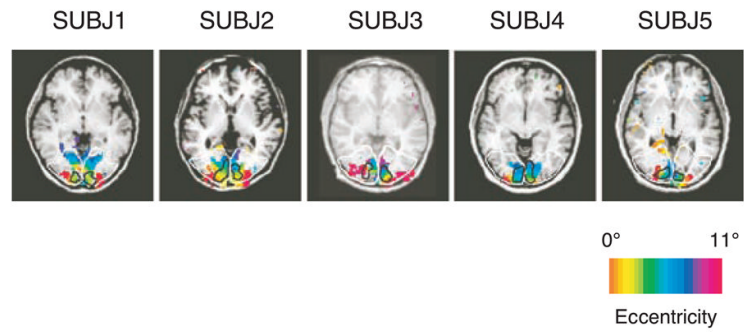


Figure 3.

The ring maps with V1 and ES (extrastriate) boundaries for 5 subjects. The eccentricity of retinotopy is color-coded according to the above scale bar. The black lines delineate the V1 boundaries, and the white lines the occipital area. ES areas are defined as the region within the occipital boundaries after excluding V1.

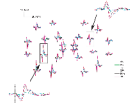


Figure 4. The mfVEP recordings for the best channel averaged across all 5 subjects. Each set of responses corresponds to the one of 24 sectors in the dartboard. The two insets show the responses at two locations on a larger scale. Dash lines indicate the signal window.

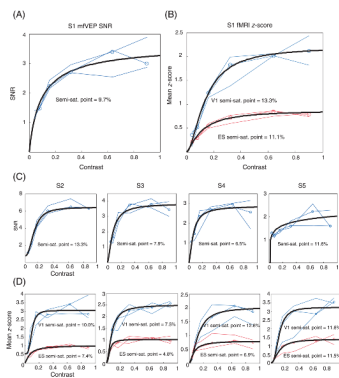


Figure 5. (A) The mfVEP contrast response functions for one subject (S1). Thin blue lines indicate the results from 3 different days. Open symbols show the median values of 3 days. Thick black curve shows the $3t$ of Equation 1. (B) The BOLD data of fMRI scanning from the same subject as in A. Thin lines indicate the mean z -scores in V1 area (blue) and ES area (red) from 3 different days. Open symbols show the median values of 3 days. Thick black curve shows the $3t$ of Equation 1. (C) (D) The mfVEP and fMRI data from the other 4 subjects.

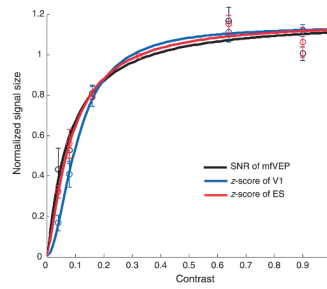


Figure 6.

The comparison of the CRFs for the mfVEP (black) and the BOLD fMRI signals from V1 (blue) and ES (red) regions. The thick lines are the best fits of Equation 1. The mean values of the 5 subjects are shown as open circles with the error bars. Note that all three curves were normalized at 32%. The error bars present one standard errors of the means shown as open circles with the error bars. Note that all three curves were normalized at 32%.

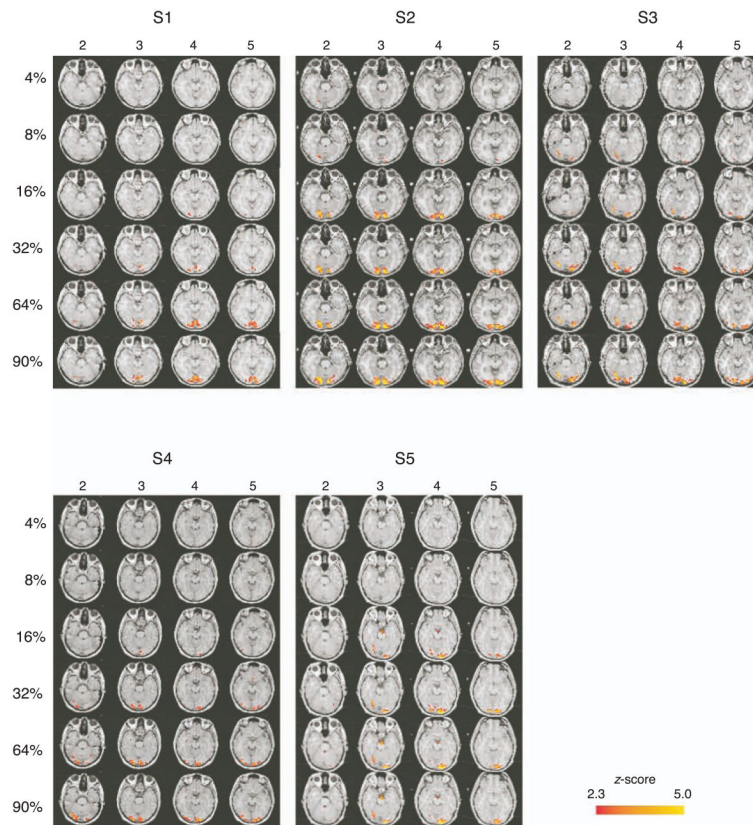


Figure 7.

The activation maps from 5 subjects. Along the rows, stimulus contrast increases, while the columns display four different slices. The slice number for each individual subject is indicated at the top of each column. Slices are contiguous, 4.5 mm thick, and increasing along the dorsal dimension. The colors indicate the increases of activation.

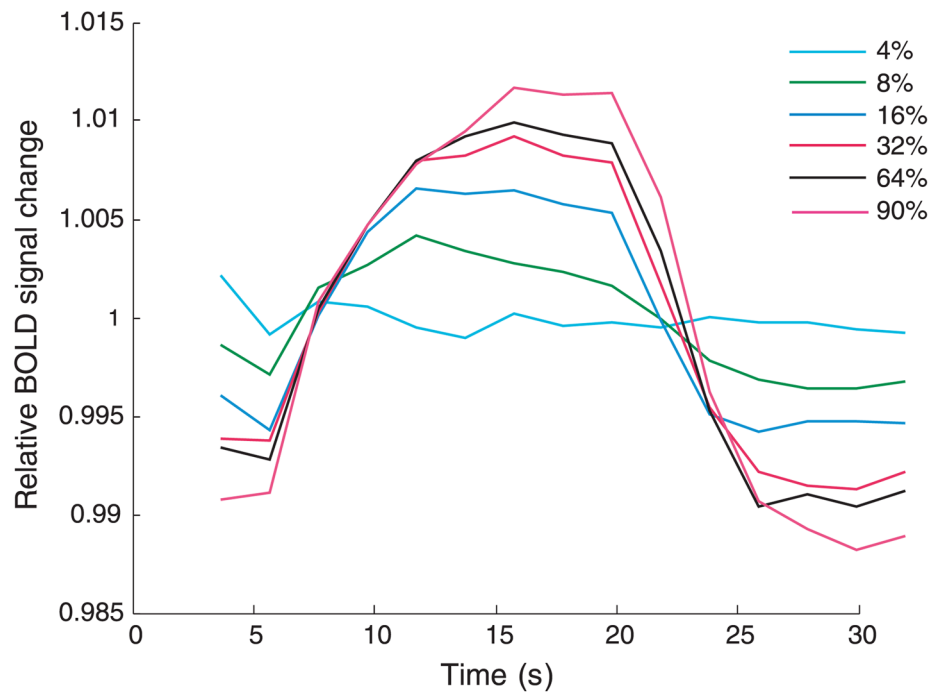


Figure 8. The time course of the BOLD response within a block. The six contrast conditions are displayed as separate lines.

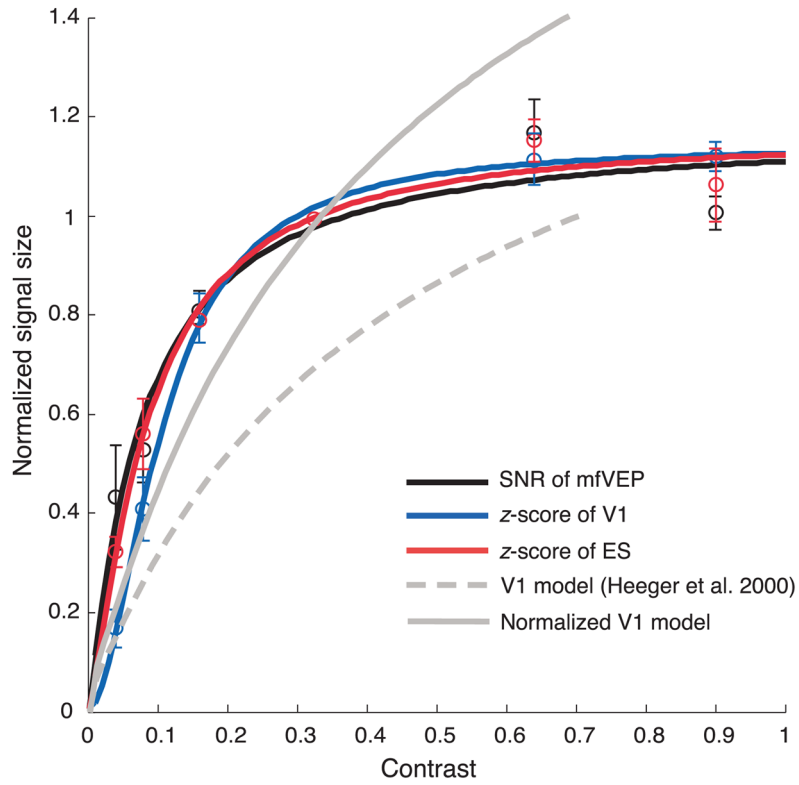


Figure 9. A comparison of the CRFs from this study and a model based upon V1 single cell recordings (Heeger et al., 2000; Hood et al., 2006). The CRFs from the mfVEP and BOLD fMRI responses from V1 and ES areas are displayed as in Figure 6. The gray curves (solid and dashed lines) are the CRFs from the V1 model of Heeger et al. (2000) pinned at the maximum response of 1.0 (dashed gray) as in Heeger et al. (2000), or at the amplitude at 32% (solid gray). The error bars present one standard errors of the means.

Table 1

The parameters of best fit for Equation 1 for the SNRs of the mfVEP versus contrast functions.

Subject	B	R_{\max}	$\sigma(\%)$	α	R^2
1	0.00	3.63	9.7	0.93	0.95
2	0.83	5.67	13.3	2.49	0.99
3	0.00	3.83	7.9	1.55	0.94
4	0.00	2.88	6.5	1.48	0.94
5	0.02	2.75	11.6	0.34	0.91
Mean \pm SE	0.17 ± 0.37	3.75 ± 1.17	9.8 ± 2.74	1.36 ± 0.80	0.95 ± 0.03
Normalized and pooled data	0.01	1.17	7.8	1.12	0.94

Table 2

The parameters of best fit for Equation 1 for the z-scores of the BOLD fMRI responses in the V1 region versus contrast functions.

Subject	B	R_{\max}	$\sigma(\%)$	α	R^2
1	0.00	2.20	14.0	1.71	0.99
2	0.54	2.50	10.0	3.65	0.96
3	0.00	2.51	7.5	1.71	0.99
4	0.00	2.02	12.6	1.82	0.99
5	0.00	3.24	11.6	2.61	0.97
Mean \pm SE	0.11 ± 0.24	2.49 ± 0.47	11.1 ± 2.5	2.3 ± 0.84	0.98 ± 0.01
Normalized & pooled data	0.00	1.14	10.7	1.88	1.00

Table 3

The parameters of best fit for Equation 1 for the z-scores of the BOLD fMRI responses in the ES region versus contrast functions.

Subject	B	R_{\max}	$\sigma(\%)$	α	R^2
1	0.01	0.87	11.1	1.37	0.98
2	0.01	1.00	7.4	1.37	0.98
3	0.01	1.00	4.8	2.20	0.94
4	0.01	0.79	6.9	1.45	0.98
5	0.01	1.04	11.5	2.15	0.99
Mean \pm SE	0.01 \pm 0	0.94 \pm 0.11	8.34 \pm 2.88	1.71 \pm 0.43	0.97 \pm 0.02
Normalized & pooled data	0.01	1.16	8.6	1.33	0.99